BELLE-CONF-0652

Search for Lepton Flavor Violating τ^- Decays into $\ell^-\eta$, $\ell^-\eta'$ and $\ell^-\pi^0$

K. Abe,[9] K. Abe,[49] I. Adachi,[9] H. Aihara,[51] D. Anipko,[1] K. Aoki,[25] T. Arakawa,[32] K. Arinstein,[1] Y. Asano,[56] T. Aso,[55] V. Aulchenko,[1] T. Aushev,[21] T. Aziz,[47] S. Bahinipati,[4] A. M. Bakich,[46] V. Balagura,[15] Y. Ban,[37] S. Banerjee,[47] E. Barberio,[24] M. Barbero,[8] A. Bay,[21] I. Bedny,[1] K. Belous,[14] U. Bitenc,[16] I. Bizjak,[16] S. Blyth,[27] A. Bondar,[1] A. Bozek,[30] M. Bračko,[23,16] J. Brodzicka,[9,30] T. E. Browder,[8] M.-C. Chang,[50] P. Chang,[29] Y. Chao,[29] A. Chen,[27] K.-F. Chen,[29] W. T. Chen,[27] B. G. Cheon,[3] R. Chistov,[15] J. H. Choi,[18] S.-K. Choi,[7] Y. Choi,[45] Y. K. Choi,[45] A. Chuvikov,[39] S. Cole,[46] J. Dalseno,[24] M. Danilov,[15] M. Dash,[57] R. Dowd,[24] J. Dragic,[9] A. Drutskoy,[4] S. Eidelman,[1] Y. Enari,[25] D. Epifanov,[1] S. Fratina,[16] H. Fujii,[9] M. Fujikawa,[26] N. Gabyshev,[1] A. Garmash,[39] T. Gershon,[9] A. Go,[27] G. Gokhroo,[47] P. Goldenzweig,[4] B. Golob,[22,16] A. Gorišek,[16] M. Grosse Perdekamp,[11,40] H. Guler,[8] H. Ha,[18] J. Haba,[9] K. Hara,[25] T. Hara,[35] Y. Hasegawa,[44] N. C. Hastings,[51] K. Hayasaka,[25] H. Hayashii,[26] M. Hazumi,[9] D. Heffernan,[35] T. Higuchi,[9] L. Hinz,[21] T. Hokuue,[25] Y. Hoshi,[49] K. Hoshina,[54] S. Hou,[27] W.-S. Hou,[29] Y. B. Hsiung,[29] Y. Igarashi,[9] T. Iijima,[25] K. Ikado,[25] A. Imoto,[26] K. Inami,[25] A. Ishikawa,[51] H. Ishino,[52] K. Itoh,[51] R. Itoh,[9] M. Iwabuchi,[6] M. Iwasaki,[51] Y. Iwasaki,[9] C. Jacoby,[21] M. Jones,[8] H. Kakuno,[51] J. H. Kang,[58] J. S. Kang,[18] P. Kapusta,[30] S. U. Kataoka,[26] N. Katayama,[9] H. Kawai,[2] T. Kawasaki,[32] H. R. Khan,[52] A. Kibayashi,[52] H. Kichimi,[9] N. Kikuchi,[50] H. J. Kim,[20] H. O. Kim,[45] J. H. Kim,[45] S. K. Kim,[43] T. H. Kim,[58] Y. J. Kim,[6] K. Kinoshita,[4] N. Kishimoto,[25] S. Korpar,[23,16] Y. Kozakai,[25] P. Križan,[22,16] P. Krokovny,[9] T. Kubota,[25] R. Kulasiri,[4] R. Kumar,[36] C. C. Kuo,[27] E. Kurihara,[2] A. Kusaka,[51] A. Kuzmin,[1] Y.-J. Kwon,[58] J. S. Lange,[5] G. Leder,[13] J. Lee,[43] S. E. Lee,[43] Y.-J. Lee,[29] T. Lesiak,[30] J. Li,[8] A. Limosani,[9] C. Y. Lin,[29] S.-W. Lin,[29] Y. Liu,[6] D. Liventsev,[15] J. MacNaughton,[13] G. Majumder,[47] F. Mandl,[13] D. Marlow,[39] T. Matsumoto,[53] A. Matyja,[30] S. McOnie,[46] T. Medvedeva,[15] Y. Mikami,[50] W. Mitaroff,[13] K. Miyabayashi,[26] H. Miyake,[35] H. Miyata,[32] Y. Miyazaki,[25] R. Mizuk,[15] D. Mohapatra,[57] G. R. Moloney,[24] T. Mori,[52] J. Mueller,[38] A. Murakami,[41] T. Nagamine,[50] Y. Nagasaka,[10] T. Nakagawa,[53] Y. Nakahama,[51] I. Nakamura,[9] E. Nakano,[34] M. Nakao,[9] H. Nakazawa,[9] Z. Natkaniec,[30] K. Neichi,[49] S. Nishida,[9] K. Nishimura,[8] O. Nitoh,[54] S. Noguchi,[26] T. Nozaki,[9] A. Ogawa,[40] S. Ogawa,[48] T. Ohshima,[25] T. Okabe,[25] S. Okuno,[17] S. L. Olsen,[8] S. Ono,[52] W. Ostrowicz,[30] H. Ozaki,[9] P. Pakhlov,[15] G. Pakhlova,[15] H. Palka,[30] C. W. Park,[45] H. Park,[20] K. S. Park,[45] N. Parslow,[46] L. S. Peak,[46] M. Pernicka,[13] R. Pestotnik,[16] M. Peters,[8] L. E. Piilonen,[57] A. Poluektov,[1] F. J. Ronga,[9] N. Root,[1] J. Rorie,[8] M. Rozanska,[30] H. Sahoo,[8] S. Saitoh,[9] Y. Sakai,[9] H. Sakamoto,[19] H. Sakaue,[34] T. R. Sarangi,[6] N. Sato,[25] N. Satoyama,[44] K. Sayeed,[4] T. Schietinger,[21] O. Schneider,[21] P. Schönmeier,[50] J. Schümann,[28] C. Schwanda,[13] A. J. Schwartz,[4] R. Seidl,[11,40] T. Seki,[53] K. Senyo,[25] M. E. Sevior,[24] M. Shapkin,[14] Y.-T. Shen,[29] H. Shibuya,[48] B. Shwartz,[1] V. Sidorov,[1] J. B. Singh,[36] A. Sokolov,[14] A. Somov,[4] N. Soni,[36] R. Stamen,[9] S. Stanič,[33]

M. Starič,[16] H. Stoeck,[46] A. Sugiyama,[41] K. Sumisawa,[9] T. Sumiyoshi,[53] S. Suzuki,[41] S. Y. Suzuki,[9] O. Tajima,[9] N. Takada,[44] F. Takasaki,[9] K. Tamai,[9] N. Tamura,[32] K. Tanabe,[51] M. Tanaka,[9] G. N. Taylor,[24] Y. Teramoto,[34] X. C. Tian,[37] I. Tikhomirov,[15] K. Trabelsi,[9] Y. T. Tsai,[29] Y. F. Tse,[24] T. Tsuboyama,[9] T. Tsukamoto,[9] K. Uchida,[8] Y. Uchida,[6] S. Uehara,[9] T. Uglov,[15] K. Ueno,[29] Y. Unno,[9] S. Uno,[9] P. Urquijo,[24] Y. Ushiroda,[9] Y. Usov,[1] G. Varner,[8] K. E. Varvell,[46] S. Villa,[21] C. C. Wang,[29] C. H. Wang,[28] M.-Z. Wang,[29] M. Watanabe,[32] Y. Watanabe,[52] J. Wicht,[21] L. Widhalm,[13] J. Wiechczynski,[30] E. Won,[18] C.-H. Wu,[29] Q. L. Xie,[12] B. D. Yabsley,[46] A. Yamaguchi,[50] H. Yamamoto,[50] S. Yamamoto,[53] Y. Yamashita,[31] M. Yamauchi,[9] Heyoung Yang,[43] S. Yoshino,[25] Y. Yuan,[12] Y. Yusa,[57] S. L. Zang,[12] C. C. Zhang,[12] J. Zhang,[9] L. M. Zhang,[42] Z. P. Zhang,[42] V. Zhilich,[1] T. Ziegler,[39] A. Zupanc,[16] and D. Zürcher[21]

(The Belle Collaboration)

[1]*Budker Institute of Nuclear Physics, Novosibirsk*
[2]*Chiba University, Chiba*
[3]*Chonnam National University, Kwangju*
[4]*University of Cincinnati, Cincinnati, Ohio 45221*
[5]*University of Frankfurt, Frankfurt*
[6]*The Graduate University for Advanced Studies, Hayama*
[7]*Gyeongsang National University, Chinju*
[8]*University of Hawaii, Honolulu, Hawaii 96822*
[9]*High Energy Accelerator Research Organization (KEK), Tsukuba*
[10]*Hiroshima Institute of Technology, Hiroshima*
[11]*University of Illinois at Urbana-Champaign, Urbana, Illinois 61801*
[12]*Institute of High Energy Physics, Chinese Academy of Sciences, Beijing*
[13]*Institute of High Energy Physics, Vienna*
[14]*Institute of High Energy Physics, Protvino*
[15]*Institute for Theoretical and Experimental Physics, Moscow*
[16]*J. Stefan Institute, Ljubljana*
[17]*Kanagawa University, Yokohama*
[18]*Korea University, Seoul*
[19]*Kyoto University, Kyoto*
[20]*Kyungpook National University, Taegu*
[21]*Swiss Federal Institute of Technology of Lausanne, EPFL, Lausanne*
[22]*University of Ljubljana, Ljubljana*
[23]*University of Maribor, Maribor*
[24]*University of Melbourne, Victoria*
[25]*Nagoya University, Nagoya*
[26]*Nara Women's University, Nara*
[27]*National Central University, Chung-li*
[28]*National United University, Miao Li*
[29]*Department of Physics, National Taiwan University, Taipei*
[30]*H. Niewodniczanski Institute of Nuclear Physics, Krakow*
[31]*Nippon Dental University, Niigata*
[32]*Niigata University, Niigata*

[33] University of Nova Gorica, Nova Gorica
[34] Osaka City University, Osaka
[35] Osaka University, Osaka
[36] Panjab University, Chandigarh
[37] Peking University, Beijing
[38] University of Pittsburgh, Pittsburgh, Pennsylvania 15260
[39] Princeton University, Princeton, New Jersey 08544
[40] RIKEN BNL Research Center, Upton, New York 11973
[41] Saga University, Saga
[42] University of Science and Technology of China, Hefei
[43] Seoul National University, Seoul
[44] Shinshu University, Nagano
[45] Sungkyunkwan University, Suwon
[46] University of Sydney, Sydney NSW
[47] Tata Institute of Fundamental Research, Bombay
[48] Toho University, Funabashi
[49] Tohoku Gakuin University, Tagajo
[50] Tohoku University, Sendai
[51] Department of Physics, University of Tokyo, Tokyo
[52] Tokyo Institute of Technology, Tokyo
[53] Tokyo Metropolitan University, Tokyo
[54] Tokyo University of Agriculture and Technology, Tokyo
[55] Toyama National College of Maritime Technology, Toyama
[56] University of Tsukuba, Tsukuba
[57] Virginia Polytechnic Institute and State University, Blacksburg, Virginia 24061
[58] Yonsei University, Seoul

Abstract

We have searched for lepton flavor violating τ decays with a pseudoscalar meson (η, η' and π^0) using a data sample of 401 fb^{-1} collected with the Belle detector at the KEKB asymmetric-energy e^+e^- collider. No evidence for these decays is found and we set the following upper limits on the branching fractions: $\mathcal{B}(\tau^- \to e^-\eta) < 9.2 \times 10^{-8}$, $\mathcal{B}(\tau^- \to \mu^-\eta) < 6.5 \times 10^{-8}$, $\mathcal{B}(\tau^- \to e^-\eta') < 1.6\times10^{-7}$, $\mathcal{B}(\tau^- \to \mu^-\eta') < 1.3\times10^{-7}$ $\mathcal{B}(\tau^- \to e^-\pi^0) < 8.0\times10^{-8}$ and $\mathcal{B}(\tau^- \to \mu^-\pi^0) < 1.2\times10^{-7}$ at the 90% confidence level, respectively. These results improve the previously published limits by factors from 2.3 to 6.4.

PACS numbers: 11.30.Fs; 13.35.Dx; 14.60.Fg

INTRODUCTION

Lepton flavor violation (LFV) is allowed in many extensions of the Standard Model (SM), such as Supersymmetry (SUSY) and leptoquark models. In particular, lepton flavor violating decays with a pseudoscalar meson ($M^0 = \eta, \eta'$ and π^0) are discussed in models with Higgs-mediated LFV processes [1], heavy singlet Dirac neutrinos [2], $R-$parity violation in SUSY [3, 4], dimension-six effective fermionic operators that induce $\tau - \mu$ mixing [5] and others [6]. The best upper limits for these modes are in the range $(1.5-10) \times 10^{-7}$ at the 90% confidence level. These were obtained by the Belle experiment using 154 fb^{-1} of data [7].

In this paper, we report a search for lepton flavor violating decays with a pseudoscalar meson $\tau^- \to \ell^- M^0$ ($\ell = e$ or μ and $M^0 = \eta, \eta'$ or π^0)[†] using 401 fb^{-1} of data collected at the $\Upsilon(4S)$ resonance and 60 MeV below it with the Belle detector at the KEKB e^+e^- asymmetric-energy collider [8].

The Belle detector is a large-solid-angle magnetic spectrometer that consists of a silicon vertex detector (SVD), a 50-layer central drift chamber (CDC), an array of aerogel threshold Čerenkov counters (ACC), a barrel-like arrangement of time-of-flight scintillation counters (TOF), and an electromagnetic calorimeter comprised of CsI(Tl) crystals (ECL), all located inside a superconducting solenoid coil that provides a 1.5 T magnetic field. An iron flux-return located outside of the coil is instrumented to detect $K^0_{\rm L}$ mesons and to identify muons (KLM). The detector is described in detail elsewhere [9].

Particle identification is very important in this measurement. We use particle identification likelihood variables based on the ratio of the energy deposited in the ECL to the momentum measured in the SVD and CDC, the shower shape in the ECL, the particle range in the KLM, the hit information from the ACC, the measured dE/dX in the CDC and the particle time-of-flight from the TOF. For lepton identification, we form likelihood ratios $\mathcal{P}(e)$ [10] and $\mathcal{P}(\mu)$ [11] based on the electron and muon probabilities, respectively, which are determined by the responses of the appropriate subdetectors.

In order to determine the event selection requirements, we use the Monte Carlo (MC) samples. The following MC programs have been used to generate background events: KORALB/TAUOLA [12] for $\tau^+\tau^-$, QQ [13] for $B\bar{B}$ and continuum, BHLUMI [14] for Bhabha events, KKMC [15] for $e^+e^- \to \mu^+\mu^-$ and AAFH [16] for two-photon processes. Signal MC is generated by KORALB/TAUOLA. Signal τ decays are two-body and assumed to have a uniform angular distribution in the τ lepton's rest frame. All kinematic variables are calculated in the laboratory frame unless otherwise specified. In particular, variables calculated in the e^+e^- center-of-mass (CM) frame are indicated by the superscript "CM".

EVENT SELECTION

We search for $\tau^+\tau^-$ events in which one τ decays into a lepton and a pseudoscalar meson on the signal side, while the other τ decays into one charged track with a sign opposite to that of the signal-side lepton and any number of additional photons and neutrinos on the tag side. Thus, the experimental signature is:

[†] Unless otherwise stated, charge conjugate decays are included throughout this paper.

$\{\tau^- \to \ell^-(= e^- \text{ or } \mu^-) + M^0(= \eta, \eta' \text{ or } \pi^0)\} + \Big\{\tau^+ \to (\text{a track})^+ + (n_\gamma^{\rm TAG} \geq 0) + X(\text{missing})\Big\}$.

We reconstruct a pseudoscalar meson in the following modes: $\eta \to \gamma\gamma$ and $\pi^+\pi^-\pi^0(\to \gamma\gamma)$, $\eta' \to \rho(\to \pi^+\pi^-)\gamma$ and $\eta(\to \gamma\gamma)\pi^+\pi^-$, $\pi^0 \to \gamma\gamma$. While the $\pi^0 \to \gamma\gamma$ and $\eta \to \gamma\gamma$ modes correspond to the 1-1 prong configuration, the other modes give 3-1 prong configurations. All charged tracks and photons are required to be reconstructed within the fiducial volume, defined by $-0.866 < \cos\theta < 0.956$, where θ is the polar angle with respect to the direction opposite to the e^+ beam. We select charged tracks with momenta transverse to the e^+ beam $p_t > 0.1$ GeV/c while the photon energies must satisfy the requirement $E_\gamma > 0.1$ GeV (0.05 GeV) for the 1-1 prong (the 3-1 prong) configuration.

Candidate τ-pair events are required to have two and four tracks with a zero net charge, for the 1-1 and 3-1 prong configurations, respectively. Event particles are separated into two hemispheres referred to as the signal and tag sides using the plane perpendicular to the thrust axis [17]. Whereas the tag side contains a single track, the signal side contains one or three tracks. For the 1-1 prong configuration, we require that the number of photons on the signal side be two or three. The track on the signal side is required to satisfy the lepton identification selection. The electron and muon identification criteria are $\mathcal{P}(e) > 0.9$ with $p > 0.7$ GeV/c and $\mathcal{P}(\mu) > 0.9$ with $p > 0.7$ GeV/c, respectively. The efficiencies for electron and muon identification after these requirements are 92% and 88%, repectively. To reduce fake pseudoscalar meson candidates, we reject radiative photons from electrons on the signal side if $\cos\theta_{e\gamma} > 0.99$.

To ensure that the missing particles are neutrinos rather than photons or charged particles that fall outside the detector acceptance, we impose additional requirements on the missing momentum vector, $\vec{p}_{\rm miss}$, calculated by subtracting the vector sum of the momenta of all tracks and photons from the sum of the e^+ and e^- beam momenta. We require that the magnitude of $\vec{p}_{\rm miss}$ be greater than 0.4 GeV/c and that its direction point into the fiducial volume of the detector. Since neutrinos are emitted only on the tag side, the direction of $\vec{p}_{\rm miss}$ should lie within the tag side of the event. The cosine of the opening angle between $\vec{p}_{\rm miss}$ and the thrust axis (on the signal side) in the CM system, $\cos\theta^{\rm CM}_{\rm tag-thrust}$, is therefore required to be less than -0.55.

Event selection for the $\eta \to \gamma\gamma$ mode

The η meson is reconstructed by combining two photons. The mass window is chosen to be 0.515 GeV/$c^2 < m_{\gamma\gamma} <$ 0.570 GeV/c^2, which corresponds to -3.0 and $+2.5$ standard deviations (σ) in terms of the mass resolution. To avoid fake η candidates, we reject those photons that form π^0 candidates in association with any other photon with $E_\gamma > 0.05$ GeV, within the π^0 mass window, 0.10 GeV/$c^2 < M_{\gamma\gamma} <$ 0.16 GeV/c^2. To suppress fake η events from beam background and initial state radiation (ISR), we require that the higher and lower energy photons in an η candidate ($E_{\gamma 1}$ and $E_{\gamma 2}$) satisfy the requirement $E_{\gamma 1} > 0.6$ GeV and $E_{\gamma 2} > 0.25$ GeV, respectively. To reduce background from Bhabha and $\mu^+\mu^-$ events, we require the momentum of a lepton and a tag-side charged particle to be less than 4.5 GeV/c.

The total visible energy in the CM frame, $E^{\rm CM}_{\rm vis}$, is defined as the sum of the energies of the η candidate, the lepton, the tag-side track (with a pion mass hypothesis) and all photon candidates. We require $E^{\rm CM}_{\rm vis}$ to satisfy the condition: 5.29 GeV $< E^{\rm CM}_{\rm vis} <$ 10.0 GeV. To

reduce background from $\mu^+\mu^-$, two-photon and Bhabha events, we further require $E_{\rm vis}^{\rm CM}$ to satisfy the veto condition: $E_{\rm vis}^{\rm CM} > 8.5$ GeV for the muon mode (electron mode) if the track on the tag side is a muon (electron). The cosine of the opening angle between the lepton and the η in the CM system, $\cos\theta_{\ell-\eta}^{\rm CM}$, is required to lie in the range $0.50 < \cos\theta_{\ell-\eta}^{\rm CM} < 0.85$. The reconstructed mass on the tag side using a track (with a pion mass hypothesis) and photons, $m_{\rm tag}$, is less than 1.777 GeV/c^2. In order to suppress background from $q\bar{q}$ ($q = u, d, s, c$) continuum events, the following requirement on the number of photon candidates on the tag side is imposed: $n^{\rm TAG} \leq 2$.

The correlation between the momentum of the track on the tag side, $p_{\rm tag}^{\rm CM}$, and the cosine of the opening angle between the thrust and missing particle, $\cos\theta_{\rm thrust-miss}^{\rm CM}$ in the CM system is employed to further suppress backgrounds from generic $\tau^+\tau^-$ and $\mu^+\mu^-$ events via the following requirements: $p_{\rm tag}^{\rm CM} > 1.1\log(\cos\theta_{\rm thrust-miss}^{\rm CM} + 0.92) + 5.5$, and $p_{\rm tag}^{\rm CM} < 5\cos\theta_{\rm thrust-miss}^{\rm CM} + 7.8$ where $p_{\rm tag}^{\rm CM}$ is in GeV/c (see Fig. 1). Finally, we require the following relation between the missing momentum $p_{\rm miss}$ and missing mass squared $m_{\rm miss}^2$ to further suppress background from generic $\tau^+\tau^-$ and continuum background. In signal events, two neutrinos are included if the τ decay on the tag side is leptonic decay, while one neutrino is included if the τ decay on the tag side is a hadronic decay. Therefore, we separate events into two classes according to the track on the tag side: leptonic or hadronic. We apply the following requirements $p_{\rm miss} > -10m_{\rm miss}^2 + 4$ and $p_{\rm miss} > 1.1m_{\rm miss}^2 - 0.3$ for a leptonic mode on the tag side, and require $p_{\rm miss} > -5m_{\rm miss}^2 - 0.25$ and $p_{\rm miss} > 2.1m_{\rm miss}^2 - 0.3$ for a hadronic mode on the tag side, where $p_{\rm tag}$ is in GeV/c (see Fig. 2). Following all the selection criteria, the signal detection efficiencies for the $\tau^- \to e^-\eta(\to \gamma\gamma)$ and $\tau^- \to \mu^-\eta(\to \gamma\gamma)$ modes are 5.08% and 7.13%, respectively.

Event selection for the $\eta \to \pi^+\pi^-\pi^0$ mode

The η meson is reconstructed from $\pi^+\pi^-\pi^0$. The π^0 candidates are formed from a pair of photons that satisfy 0.115 GeV/$c^2 < M_{\gamma\gamma} <$ 0.152 GeV/c^2 ($\pm 2.5\sigma$). with $p_{\pi^0} > 0.1$ GeV/c, where p_{π^0} is the π^0 momentum in the laboratory system. The mass window for $\eta \to \pi^+\pi^-\pi^0$ is chosen as 0.532 GeV/$c^2 < M_{3\pi} <$ 0.562 GeV/c^2, which corresponds to $\pm 3.0\sigma$. Figure 3 shows the mass distribution for the $\eta \to \pi^+\pi^-\pi^0$ candidates. Good agreement between data and the MC expectation is observed.

Similarly for the $\eta(\to \gamma\gamma)$ mode, we require the following: 5.29 GeV $< E_{\rm vis}^{\rm CM} <$10.0 GeV, $0.50 < \cos\theta_{\ell-\eta}^{\rm CM} < 0.85$ (see Fig. 4 (a) and (b)) and $m_{\rm tag} <$ 1.777 GeV/c^2. The requirement on the number of the photon candidates for the signal is $n^{\rm SIG} \leq 1$. In addition we apply the following requirements: $p_{\rm miss} > -5m_{\rm miss}^2 - 0.25$ and $p_{\rm miss} > 2.1m_{\rm miss}^2 - 0.3$ for hadronic tags, and $p_{\rm miss} > -10m_{\rm miss}^2 - 4$ and $p_{\rm miss} > 1.1m_{\rm miss}^2 - 1$ for leptonic tags, respectively. After all the selection criteria, the signal detection efficiencies for the $\tau^- \to e^-\eta(\to \pi^+\pi^-\pi^0)$ and $\tau^- \to \mu^-\eta(\to \pi^+\pi^-\pi^0)$ modes are 5.25% and 7.60%, respectively.

Event selection for the $\eta' \to \rho(\to \pi^+\pi^-)\gamma$ mode

For the $\rho \to \pi^+\pi^-$ selection, the mass window is chosen to be 0.550 GeV/$c^2 < m_{\pi\pi} <$ 0.900 GeV/c^2. We reconstruct η' candidates using a ρ candidate and a photon on the signal side. The η' mass window is chosen to be 0.930 GeV/$c^2 < m_{\rho\gamma} <$ 0.970 GeV/c^2, which corresponds to -3.0 and $+2.5\sigma$. Furthermore, we veto photons from π^0 candidates in order

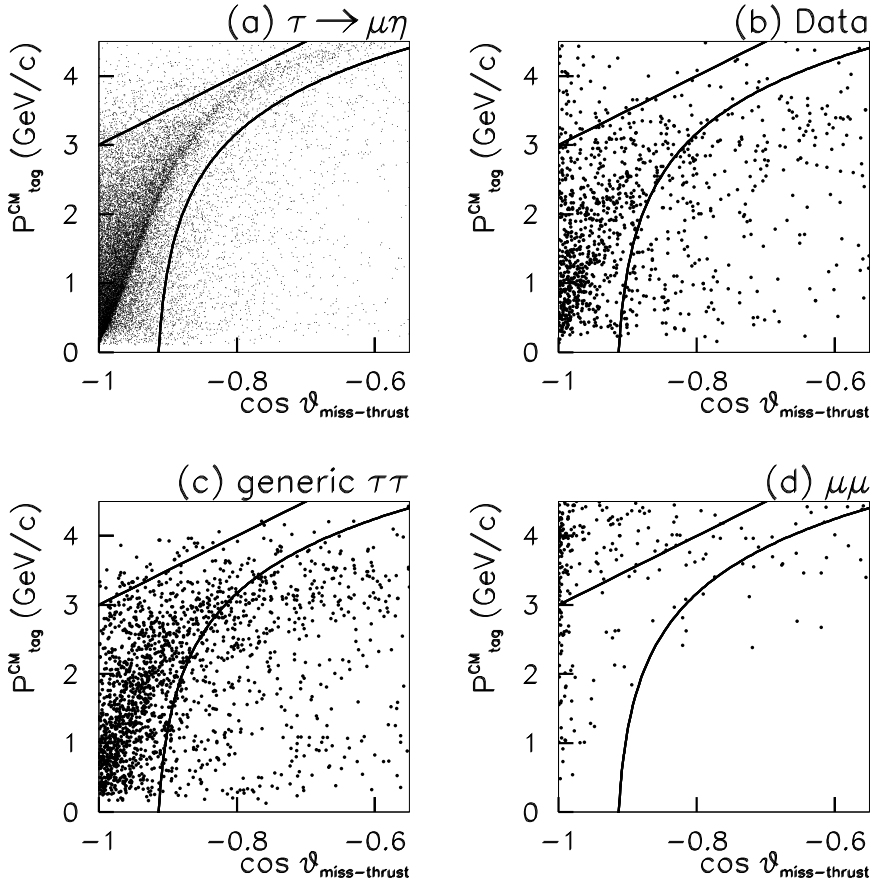

FIG. 1: Scatter-plots of (a) signal MC ($\tau^- \to \mu^-\eta(\to \gamma\gamma)$), (b) data, (c) generic $\tau^+\tau^-$ MC events and (d) $\mu^+\mu^-$ MC events on the $p^{\rm CM}_{\rm tag}$ vs $\cos\theta_{\rm miss-thrust}$ plane. Selected regions are indicated by the curves with arrows.

to avoid fake η' candidates from $\pi^0 \to \gamma\gamma$. We remove events if a π^0 with invariant mass in the range 0.10 GeV/c^2 $< M_{\gamma\gamma} <$ 0.16 GeV/c^2 is reconstructed by a photon from the η' candidate and another photon with $E_\gamma > 0.05$ GeV. Figure 5 shows the $\rho \to \pi^+\pi^-$ and $\eta' \to \rho\gamma$ mass distributions. Dominant backgrounds for this mode come from $\tau^- \to h^-\rho^0\nu_\tau(+\pi^0)$ with a photon from π^0 decay, beam background and ISR. As shown in Fig. 5, we see no η' peak either in data or in MC since decay modes with an η' are very rare and are not included in the generic τ decay model [18].

To suppress fake candidates from beam background and ISR, we require the photon energy to be greater than 0.25 GeV for the barrel and 0.40 GeV for the forward region. Similar to the η mode, we require the following: 5.29 GeV $< E^{\rm CM}_{\rm vis} <$11.0 GeV, $m_{\rm tag} <$ 1.777 GeV/c^2, $0.50 < \cos\theta^{\rm CM}_{\ell-\eta'}$ (see Fig. 6 (a), (b) and (c)). The requirement on the number of the photon candidates for the signal is $n^{\rm SIG} \leq 1$, (see Fig. 6 (d)). We apply the following requirements $p_{\rm miss} > -5m^2_{\rm miss} - 0.2$ and $p_{\rm miss} > 2m^2_{\rm miss} - 0.3$ for hadronic tags, and $p_{\rm miss} > -8m^2_{\rm miss} - 0.2$ and $p_{\rm miss} > 1.2m^2_{\rm miss} - 0.3$ for leptonic tags, respectively. Following all the selection criteria, the signal detection efficiencies for the electron and muon modes are 5.28% and 6.00%, respectively.

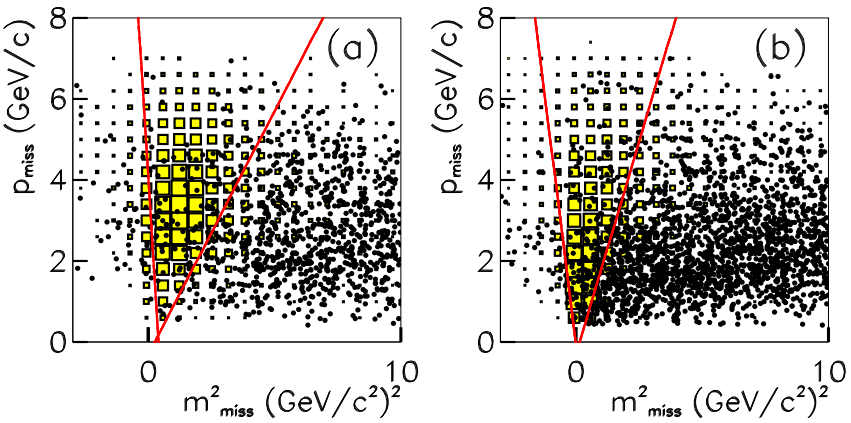

FIG. 2: Scatter-plots of missing momentum, $p_{\rm miss}$, vs missing mass squared, $m^2_{\rm miss}$, for (a) leptonic and (b) hadronic tags. Selected regions are indicated by lines. The data are the dots. The filled boxes show the signal MC ($\tau^- \to \mu^- \eta$) distribution with arbitrary normalization.

Event selection for the $\eta' \to \eta(\to \gamma\gamma)\pi^+\pi^-$ mode

For η meson reconstruction, we apply the same selection criteria as in the $\tau \to \ell\eta(\to \gamma\gamma)$ analysis. The $\eta \to \gamma\gamma$ mass window is chosen to be $0.515\ {\rm GeV}/c^2 < m_{\gamma\gamma} < 0.570\ {\rm GeV}/c^2$ and we reject photons from π^0 decay. Next, we reconstruct η' candidates using an η candidate and two oppositely charged tracks consistent with being pions. We require $P(e) < 0.1$ for both tracks in the η' candidate. The η' mass window is chosen to be $0.920\ {\rm GeV}/c^2 < m_{\eta\pi^+\pi^-} < 0.980\ {\rm GeV}/c^2$, which corresponds to $\pm 3.0\sigma$.

We apply the same cuts on $\cos\theta^{\rm CM}_{\rm thrust-miss}$, $E^{\rm CM}_{\rm vis}$, $\cos\theta^{\rm CM}_{\ell-\eta'}$, the invariant mass on the tag side, the number of photons on the signal side and $m^2_{\rm miss}$ vs. $p_{\rm miss}$ cut as on the $\eta' \to \rho\gamma$ analysis. We also impose the following requirements: $p_{\rm miss} > -4m^2_{\rm miss} - 0.8$ and $p_{\rm miss} > 2.5m^2_{\rm miss} - 0.2$ for hadronic tags, and $p_{\rm miss} > -3m^2_{\rm miss}$ and $p_{\rm miss} > 1.5m^2_{\rm miss} - 0.5$ for leptonic tags, respectively, where $p_{\rm tag}$ is in GeV/c. Following all the selection criteria, the signal detection efficiencies for the electron and muon modes are 4.75% and 5.47%, respectively.

Event selection for the $\pi^0(\to \gamma\gamma)$ modes

The π^0 candidate is required to satisfy the condition $0.115\ {\rm GeV}/c^2 < M_{\gamma\gamma} < 0.152\ {\rm GeV}/c^2$ with $p_{\pi^0} > 0.1$ GeV/c on the signal side. We require the same cuts as for the $\eta(\to \gamma\gamma)$ mode since the final state is the same. We change the photon energy thresholds for the π^0 candidate $E_{\gamma 1} > 0.90$ GeV, $E_{\gamma 2} > 0.20$ GeV and $p_\ell > 1.5$ GeV/c compared to $\tau \to \ell\eta(\to \gamma\gamma)$ (shown in Fig. 7 (a), (b) and (c)). Furthermore, the opening angle between ℓ and π^0 in the CM system ($\cos\theta^{CM}_{\ell\pi^0}$) should be in the range $0.5 < \cos\theta^{CM}_{\ell\pi^0} < 0.8$ (shown in Fig. 7 (d)). Following all the selection criteria, the signal detection efficiencies for the electron and muon modes are 4.35% and 5.03%, respectively.

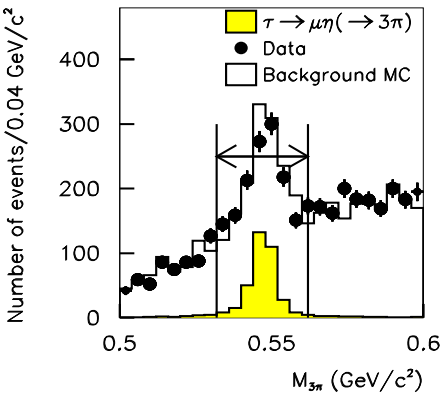

FIG. 3: Invariant mass distribution of $\eta \to \pi^+\pi^-\pi^0$ candidates. While the signal MC ($\tau^- \to \mu^-\eta(\to \pi^+\pi^-\pi^0)$) distribution is normalized arbitrarily, the data and background MC are normalized to the same luminosity. The selected region is indicated by arrows between the vertical lines

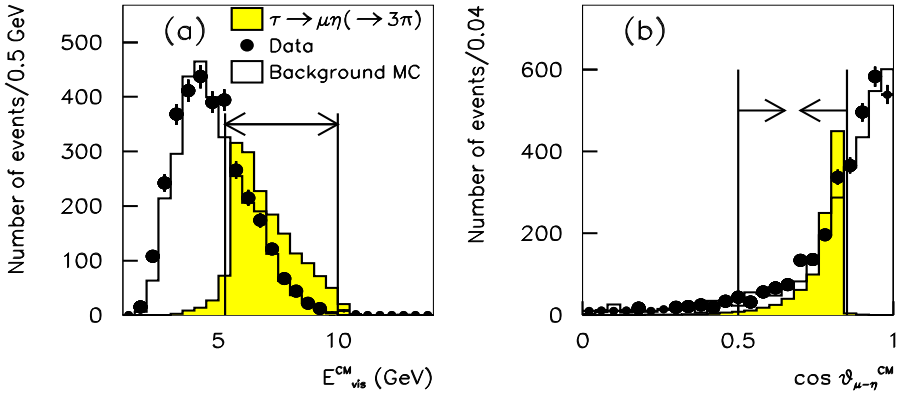

FIG. 4: Kinematic distributions used in the event selection after the initial $\eta \to \pi^+\pi^-\pi^0$ selection, muon identification and missing particles requirements: (a) The total visible energy in the CM frame; (b) the opening angle between the muon and η candidate in the CM frame; while the signal MC ($\tau^- \to \mu^-\eta(\to \pi^+\pi^-\pi^0)$) distribution is normalized arbitrarily, the data and background MC are normalized to the same luminosity. Selected regions are indicated by the arrows between the vertical lines.

SIGNAL REGION AND BACKGROUND ESTIMATION

Signal candidates are examined in the two-dimensional plots of the $\ell^- M^0$ invariant mass, $M_{\rm inv}$, and the difference of their energy from the beam energy in the CM system, ΔE. A signal event should have $M_{\rm inv}$ close to the τ-lepton mass and ΔE close to zero. For all modes, the $M_{\rm inv}$ and ΔE resolutions are parameterized from the MC distributions with asymmetric Gaussian shapes to account for initial state radiation and ECL energy leakage for photons. The resolutions in $M_{\rm inv}$ and ΔE are given in Table I.

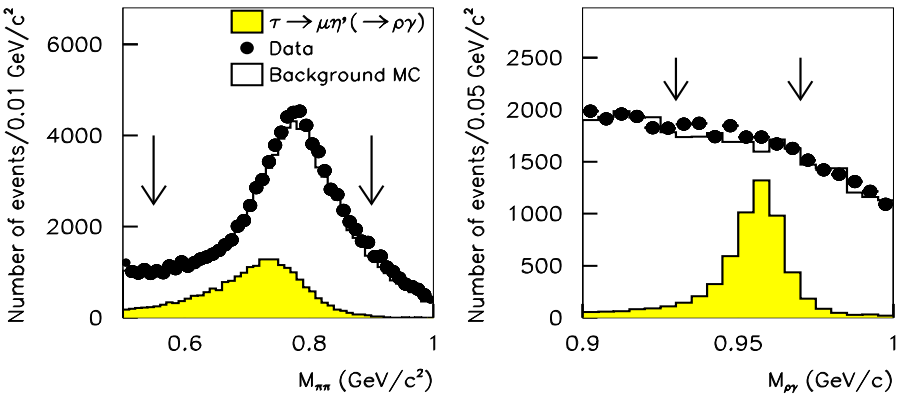

FIG. 5: The $\rho \to \pi^+\pi^-$ (left) and $\eta' \to \rho\gamma$ (right) mass distributions. While the signal MC ($\tau^- \to \mu^-\eta'$) distribution is normalized arbitrarily, the data and background MC are normalized to the same luminosity. Selected regions are indicated by the arrows.

Mode	$\sigma^{\rm high}_{M_{\rm inv}}$ (MeV/c^2)	$\sigma^{\rm low}_{M_{\rm inv}}$ (MeV/c^2)	$\sigma^{\rm high}_{\Delta E}$ (MeV)	$\sigma^{\rm low}_{\Delta E}$ (MeV)
$\mu\eta(\to \gamma\gamma)$	14.7	19.4	30.3	61.4
$\mu\eta(\to \pi^+\pi^-\pi^0)$	7.2	8.5	18.5	36.4
$e\eta(\to \gamma\gamma)$	14.0	19.8	37.3	62.4
$e\eta(\to \pi^+\pi^-\pi^0)$	7.6	9.3	19.4	41.8
$\mu\eta'(\to \rho\gamma)$	7.8	9.0	16.8	34.1
$\mu\eta'(\to \eta\pi^+\pi^-)$	11.2	19.1	27.1	53.5
$e\eta'(\to \rho\gamma)$	9.2	10.4	19.6	40.0
$e\eta'(\to \eta\pi^+\pi^-)$	10.3	21.9	26.1	59.4
$\mu\pi^0$	14.9	19.1	33.8	63.0
$e\pi^0$	12.7	23.1	35.6	64.6

TABLE I: Summary of $M_{\rm inv}$ (MeV/c^2) and ΔE resolutions (MeV)

To evaluate the branching fraction, we use elliptical regions, which contain 90% of the MC signal that satisfies all cuts. We find that an elliptical signal region gives better sensitivity than a rectangular one. The signal regions are shown in Fig. 8; the corresponding signal efficiencies are given in Table II.

We blind the signal region so as not to bias our choice of selection criteria. Figures 8 and 9 show scatter-plots for data and signal MC samples distributed over $\pm 10\sigma$ in the $M_{\rm inv} - \Delta E$ plane. As there are few remaining MC background events in the signal ellipse, we estimate the background contribution using the $M_{\rm inv}$ sideband regions. Extrapolation to the signal region assumes that the background distribution is flat along the $M_{\rm inv}$ axis. We then estimate the expected number of the background events in the signal region for each mode using the number of data events observed in the sideband region inside the horizontal lines but excluding the signal region as shown in Fig. 8 and 9. The numbers of background events in the 90% elliptical signal region are also shown in Table II.

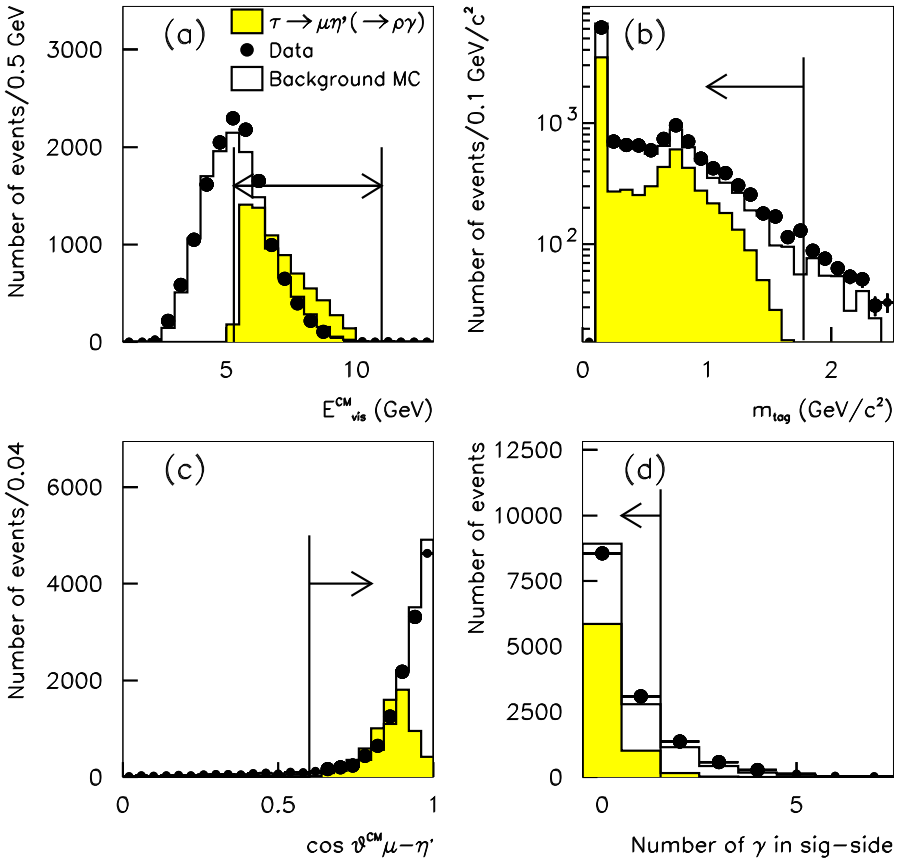

FIG. 6: Kinematic distributions used in the event selection after $\eta' \to \rho\gamma$ selection, muon identification and missing particles requirements: (a) the total energy in the CM frame; (a) the invariant mass on the tag side; (c) the opening angle between the missing particle and tag-side track in the CM frame; (d) the number of photons on the signal side. While the signal MC ($\tau^- \to \mu^-\eta'(\to \rho\gamma)$) distribution is normalized arbitrarily, the data and background MC are normalized to the same luminosity. Selected regions are indicated by arrows from the marked cut boundaries.

Systematic uncertainties for M^0 reconstruction are 3.0%, 4.0%, 4.0%, 5.0% and 3.0% for $\eta \to \gamma\gamma$, $\eta \to \pi^+\pi^-\pi^0$, $\eta' \to \rho\gamma$, $\eta' \to \eta\pi^+\pi^-$ and $\pi^0 \to \gamma\gamma$, respectively. Furthermore, the uncertainties due to the branching ratios of the M^0 meson are 0.7%, 1.8%, 3.4% and 3.5% for $\eta \to \gamma\gamma$, $\eta \to \pi^+\pi^-\pi^0$, $\eta' \to \rho\gamma$ and $\eta' \to \eta\pi^+\pi^-$, respectively [18]. For the π^0 veto we take a 5.5% uncertainty for $\eta \to \gamma\gamma$ while a 2.8% uncertainty is assigned to the $\eta' \to \rho\gamma$ mode. The uncertainties in the trigger (0.5−1.0%), tracking (2.0%), lepton identification (2.0%), MC statistics (1.0−1.5%), luminosity (1.4%) are also considered. All these uncertainties are added in quadrature, and the total systematic uncertainties are shown in Table II.

While the angular distribution of signal τ decays is initially assumed to be uniform in this analysis, it is sensitive to the lepton flavor violating interaction structure [19]. The spin correlation between the τ lepton on the signal and that on the tag side must be considered. A possible nonuniformity was taken into account by comparing the uniform case with MC's assuming $V - A$ and $V + A$ interactions, which result in the maximum possible variations.

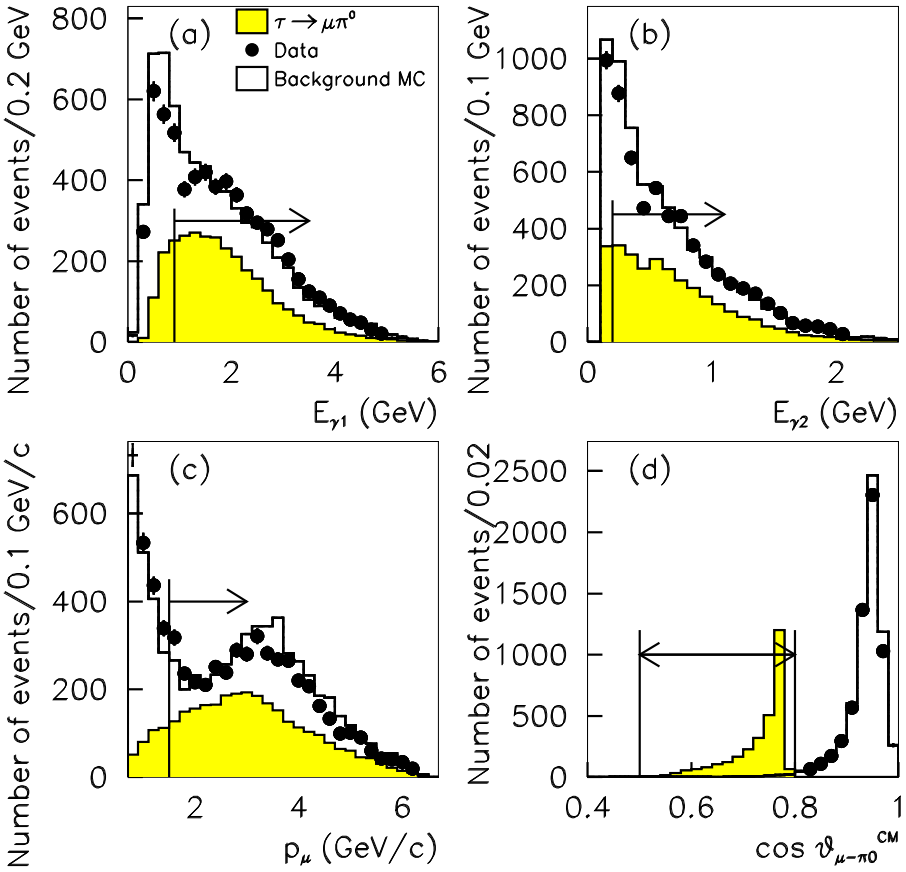

FIG. 7: Kinematic distributions used in the event selection: (a) higher energy and (b) lower energy of a photon from the π^0 candidate ($E_{\gamma 1}$ and $E_{\gamma 2}$); (c) momentum of a muon (p_μ); (d) the cosine of the opening angle between the muon and π^0 in the CM frame ($\cos\theta^{\rm CM}_{\mu-\pi^0}$). While the signal MC ($\tau^- \to \mu^-\pi^0$) distribution is normalized arbitrarily, the data and background MC are normalized to the same luminosity. Selected regions are indicated by arrows from the marked cut boundaries.

No statistically significant difference in the $M_{\rm inv}$ – ΔE distribution or the efficiencies is found compared to the case of the uniform distribution. Therefore, systematic uncertainties due to these effects are neglected in the upper limit evaluation.

We open the blind and find no data events in the blinded region after event selection. Only in the case of $\tau \to \mu\pi^0(\to \gamma\gamma)$, one event is found in the elliptical region. Since no statistically significant excess of data over the expected background in the signal region is observed, we set upper limits for branching fractions. The upper limit on the number of signal events at the 90% confidence level (C.L.) s_{90} including systematic uncertainty is obtained with the use of the Feldman-Cousins method [20] calculated by the POLE program without conditioning [21]. The upper limit on the branching fraction ($\mathcal{B}$) is then calculated as

$$\mathcal{B}(\tau^- \to \ell^- M^0) < \frac{s_{90}}{2N_{\tau\tau}\varepsilon\mathcal{B}_{M^0}} \qquad (1)$$

Mode	$\mathcal{B}_{M^0}$	ε	b_0	s	Total Sys.	s_{90}
$\tau \to \mu\eta(\to \gamma\gamma)$	0.3943	6.42%	0.40±0.29	0	7.1%	2.1
$\tau \to \mu\eta(\to \pi^+\pi^-\pi^0)$	0.226	6.84%	0.24±0.24	0	5.6%	2.2
$\tau \to e\eta(\to \gamma\gamma)$	0.3943	4.57%	0.25±0.25	0	7.1%	2.2
$\tau \to e\eta(\to \pi^+\pi^-\pi^0)$	0.226	4.72%	0.53±0.53	0	5.6 %	2.0
$\tau \to \mu\eta'(\to \rho\gamma)$	0.295×1.0	5.40%	0.23±0.23	0	6.8%	2.2
$\tau \to \mu\eta'(\to \eta\pi^+\pi^-)$	0.443×0.3943	4.92%	$0.0^{+0.23}_{-0.0}$	0	8.9%	2.5
$\tau \to e\eta'(\to \rho\gamma)$	0.295×1.0	4.76%	$0.0^{+0.33}_{-0.0}$	0	6.8%	2.5
$\tau \to e\eta'(\to \eta\pi^+\pi^-)$	0.443×0.3943	4.27%	$0.0^{+0.24}_{-0.0}$	0	8.9%	2.5
$\tau \to \mu\pi^0(\to \gamma\gamma)$	0.98798	4.53%	0.58±0.34	1	4.5%	3.8
$\tau \to e\pi^0(\to \gamma\gamma)$	0.98798	3.93%	0.20±0.20	0	4.5%	2.2

TABLE II: Results of the final event selection for the individual modes: $\mathcal{B}_{M^0}$ is the branching fraction for the M^0 decay; b_0 and s are the number of expected background and observed events in the signal region, respectively; "Total sys." means the total systematic uncertainty; $s_{90\%}$ is the upper limit on the number of signal events including systematic uncertainties.

Mode	M^0 subdecay mode	Upper limit of $\mathcal{B}$ at 90%C.L.
$\tau^- \to \mu^-\eta$	$\eta \to \gamma\gamma$	1.2×10^{-7}
	$\eta \to \pi^+\pi^-\pi^0$	2.0×10^{-7}
	Combined	6.5×10^{-8}
$\tau^- \to e^-\eta$	$\eta \to \gamma\gamma$	1.7×10^{-7}
	$\eta \to \pi^+\pi^-\pi^0$	2.6×10^{-7}
	Combined	9.2×10^{-8}
$\tau^- \to \mu^-\eta'$	$\eta \to \rho\gamma$	1.9×10^{-7}
	$\eta \to \eta\pi^+\pi^-$	4.1×10^{-7}
	Combined	1.3×10^{-7}
$\tau^- \to e^-\eta'$	$\eta \to \rho\gamma$	2.5×10^{-7}
	$\eta \to \eta\pi^+\pi^-$	4.7×10^{-7}
	Combined	1.6×10^{-7}
$\tau^- \to \mu^-\pi^0$	$\pi^0 \to \gamma\gamma$	1.2×10^{-7}
$\tau^- \to e^-\pi^0$	$\pi^0 \to \gamma\gamma$	8.0×10^{-8}

TABLE III: Summary of upper limits on $\mathcal{B}$ at 90%C.L.

where $\mathcal{B}_{M^0}$ is taken from PDG [18] and $N_{\tau\tau} = 357.7\times10^6$ is the number of $\tau-$pairs produced in 401 fb^{-1} of data. We obtain $N_{\tau\tau}$ using $\sigma_{\tau\tau} = 0.892 \pm 0.002$ nb, the $e^+e^- \to \tau^+\tau^-$ cross section at the $\Upsilon(4S)$ resonance calculated by KKMC [15]. The upper limits for the branching fractions are in the range $\mathcal{B}(\tau^- \to \ell^- M^0) < (6.5 - 16) \times 10^{-8}$ at the 90% confidence level, respectively. A summary of the upper limits is given in Table III. These results improve the previously published limits [7] by factors of 2.3−6.4.

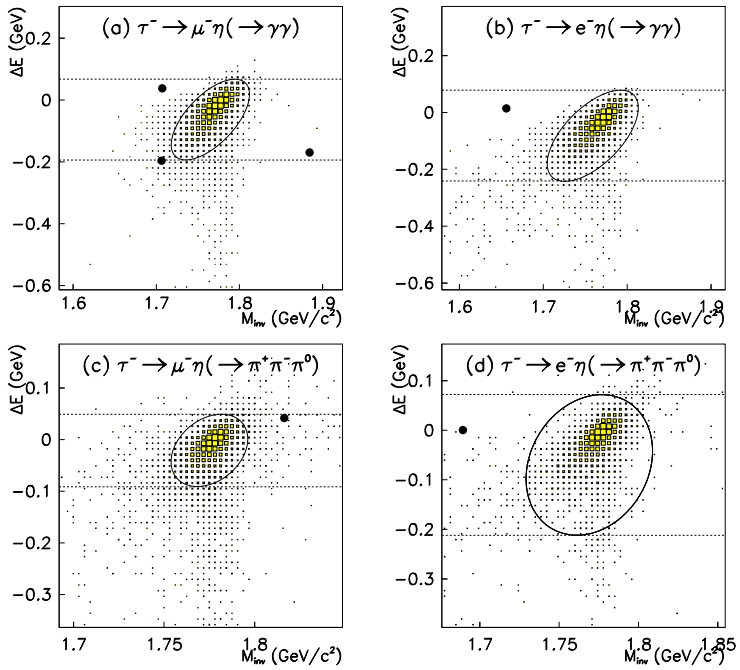

FIG. 8: Scatter-plots of data in the $M_{\rm inv}$ – ΔE plane: (a), (b), (c) and (d) correspond to the $\pm 10\sigma$ area for the $\tau^- \to \mu^- \eta(\to \gamma\gamma)$, $\tau^- \to e^- \eta(\to \gamma\gamma)$, $\tau^- \to \mu^- \eta(\to \pi^+\pi^-\pi^0)$ and $\tau^- \to e^- \eta(\to \pi^+\pi^-\pi^0)$, modes, respectively. The filled boxes show the MC signal distribution with arbitrary normalization. The elliptical signal region shown by the solid curve is used for evaluating the signal yield. The region between the horizontal lines excluding the signal region is used to estimate the expected background in the elliptical region.

DISCUSSION

The branching ratio for the $\tau^- \to \mu^- \eta$ mode is enhanced by Higgs-mediated LFV if large mixing between a left-hand scalar muon and scalar tau in the corresponding SUSY model occurs [1] and can be written as

$$\mathcal{B}(\tau^- \to \mu^- \eta) = 8.4 \times 10^{-7} \left(\frac{\tan\beta}{60}\right)^6 \left(\frac{100\mathrm{GeV}/c^2}{m_A}\right)^4, \qquad (2)$$

where m_A is the pseudoscalar Higgs mass and $\tan\beta$ is the ratio of the vacuum expectation values. From our upper limit on the branching fraction for the $\tau^- \to \mu^- \eta$ decay, some region of m_A and $\tan\beta$ parameters can be excluded. Figure 10 shows the excluded region in the m_A vs $\tan\beta$ plane. Figure 10 also shows the constraints at 95% C.L. from the CDF [22], DØ [23] and LEP2 experiments [24]. The excluded regions from the CDF, DØ and LEP2 experiments are shown with $\mu > 0$ and $m_h^{\rm max}$. Our result has a sensitivity competitive with that of the CDF and DØ experiments, which searched for $p\bar{p} \to \phi b(\bar{b})$ and $\tau^+\tau^-$ events, where ϕ is a neutral Higgs boson in the minimal supersymmetric standard model ($\phi = h, H$ and A).

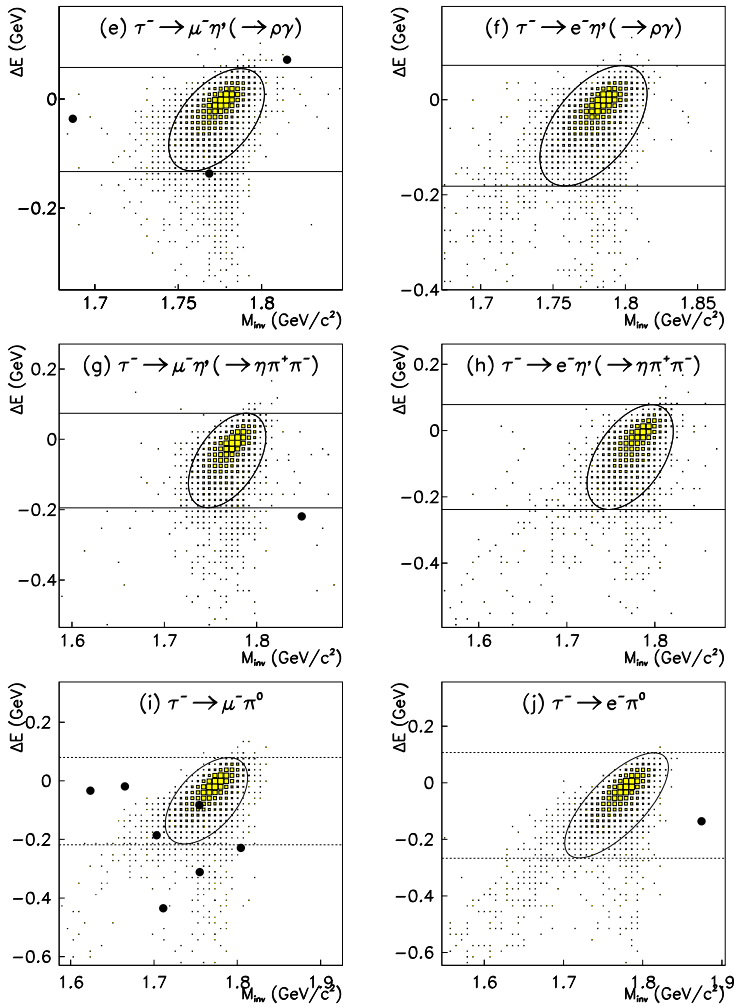

FIG. 9: Scatter-plots of data in the $M_{\rm inv}$ – ΔE plane: (e), (f), (g), (h), (i) and (j) correspond to the $\pm 10\sigma$ area for the $\tau^- \to \mu^- \eta'(\to \rho\gamma)$, $\tau^- \to e^- \eta'(\to \rho\gamma)$, $\tau^- \to \mu^- \eta'(\to \eta\pi^+\pi^-)$, $\tau^- \to e^- \eta'(\to \eta\pi^+\pi^-)$, $\tau^- \to \mu^- \pi^0(\to \gamma\gamma)$ and $\tau^- \to e^- \pi^0(\to \gamma\gamma)$ modes, respectively. The data are indicated by the solid circles. The filled boxes show the MC signal distribution with arbitrary normalization. The elliptical signal region shown by the solid curve is used for evaluating the signal yield. The region between the horizontal lines excluding the signal region is used to estimate the expected background in the elliptical region.

SUMMARY

We have searched for lepton flavor violating τ decays with a pseudoscalar meson (η, η' and π^0) using 401 fb^{-1} of data. No signal is found and we set the following upper limits of the branching fractions: $\mathcal{B}(\tau^- \to e^- \eta) < 9.2 \times 10^{-8}$, $\mathcal{B}(\tau^- \to \mu^- \eta) < 6.5 \times 10^{-8}$, $\mathcal{B}(\tau^- \to e^- \eta') < 1.6 \times 10^{-7}$, $\mathcal{B}(\tau^- \to \mu^- \eta') < 1.3 \times 10^{-7}$ $\mathcal{B}(\tau^- \to e^- \pi^0) < 8.0 \times 10^{-8}$ and $\mathcal{B}(\tau^- \to \mu^- \pi^0) < 1.2 \times 10^{-7}$ at the 90% confidence level, respectively. These results improve the previously published limits by factors from 2.3 to 6.4 and help to constrain

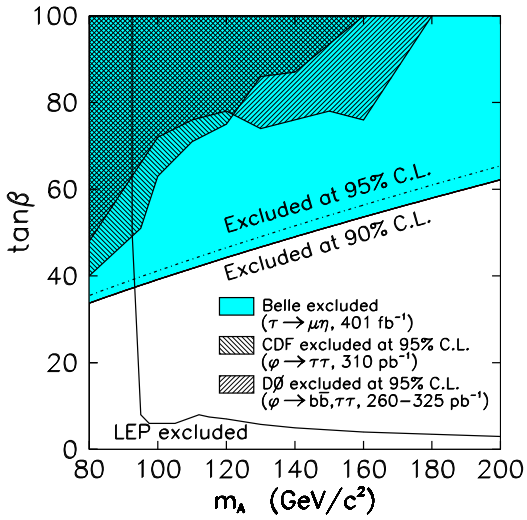

FIG. 10: The excluded region in the m_A vs $\tan\beta$ plane from our results at 90% C.L. and other experiments at 95% C.L. from CDF [22], DØ [23], LEP [24]. The excluded regions from the CDF, DØ and LEP2 experiments are shown with $\mu > 0$ and $m_h^{\max}$.

physics beyond the Standard Model.

Acknowledgments

We thank the KEKB group for the excellent operation of the accelerator, the KEK cryogenics group for the efficient operation of the solenoid, and the KEK computer group and the National Institute of Informatics for valuable computing and Super-SINET network support. We acknowledge support from the Ministry of Education, Culture, Sports, Science, and Technology of Japan and the Japan Society for the Promotion of Science; the Australian Research Council and the Australian Department of Education, Science and Training; the National Science Foundation of China and the Knowledge Innovation Program of the Chinese Academy of Sciencies under contract No. 10575109 and IHEP-U-503; the Department of Science and Technology of India; the BK21 program of the Ministry of Education of Korea, the CHEP SRC program and Basic Research program (grant No. R01-2005-000-10089-0) of the Korea Science and Engineering Foundation, and the Pure Basic Research Group program of the Korea Research Foundation; the Polish State Committee for Scientific Research; the Ministry of Science and Technology of the Russian Federation; the Slovenian Research Agency; the Swiss National Science Foundation; the National Science Council and the Ministry of Education of Taiwan; and the U.S. Department of Energy.

[1] M. Sher, Phys. Rev. D **66**, 057301 (2002).
[2] A. Ilakovac, Phys. Rev. D **62**, 036010 (2000).
[3] J. P. Saha and A. Kundu, Phys. Rev. D **66**, 054021 (2002).
[4] R. Barbier *et al.*, Phys. Rep. **420**, 1 (2005).
[5] D. Black *et al.*, Phys. Rev. D **66**, 053002 (2002).
[6] W. j. Li, Y. d. Yang and X. d. Zhang, Phys. Rev. D **73**, 073005 (2006).
[7] Y. Enari *et al.* (Belle Collaboration), Phys. Lett. B **622**, 218 (2005).
[8] S. Kurokawa and E. Kikutani, Nucl. Instr. and Meth. A **499**, 1 (2003), and other papers included in this Volume.
[9] A. Abashian *et al.* (Belle Collaboration), Nucl. Instr. and Meth. A **479**, 117 (2002).
[10] K. Hanagaki *et al.*, Nucl. Instr. and Meth. A **485**, 490 (2002).
[11] A. Abashian *et al.*, Nucl. Instr. and Meth. A **491**, 69 (2002).
[12] S. Jadach and Z. Wąs, Comp. Phys. Commun. **85**, 453 (1995).
[13] QQ is an event generator developed by the CLEO Collaboration and described in http://www.lns.cornell.edu/public/CLEO/soft/QQ/. It is based on the LUND Monte Carlo for jet fragmentation and e^+e^- physics described in T. Sjöstrand, Comp. Phys. Commun. **39**, 347 (1986) and T. Sjöstrand, Comp. Phys. Commun. **43**, 367 (1987).
[14] S. Jadach *et al.*, Comp. Phys. Commun. **79**, 305 (1992).
[15] S. Jadach *et al.*, Comp. Phys. Commun. **130**, 260 (2000).
[16] F. A. Berends *et al.*, Comp. Phys. Commun. **40**, 285 (1986).
[17] S. Brandt *et al.*, Phys. Lett. **12**, 57 (1964); E. Farhi, Phys. Rev. Lett. **39**, 1587 (1977).
[18] S. Eidelman *et al.* (Particle Data Group), Phys. Lett. B **592**, 1 (2004).
[19] R. Kitano and T. Okada, Phys. Rev. D **63**, 3873 (2001).
[20] G. J. Feldman and R.D. Cousins, Phys. Rev. D **57**, 3873 (1998).
[21] See http://www3.tsl.uu.se/~cornad/pole.html, J. Conrad *et al.*, Phys. Rev. D **67**, 012002 (2003).
[22] A. Abulencia *et al.* (CDF Collaboration), Phys. Rev. Lett. **96**, 011802 (2006).
[23] V. M. Abazov *et al.* (DØ Collaboration), Phys. Rev. Lett. **95**, 151801 (2005); V. M. Abazov *et al.* (DØ Collaboration), hep-ex/0605009.
[24] The ALEPH, DELPHI, L3 and OPAL Collaboration, LEP Higgs Working Group, LHWG-Note 2005-01, http://lephiggs.web.cern.ch/LEPHIGGS/papers/July2005_MSSM/.